

Article

Pestalotiopols E–J, Six New Polyketide Derivatives from a Marine Derived Fungus *Pestalotiopsis* sp. SWMU-WZ04-1

Liyuan Jiang¹, Baorui Teng¹, Mengyu Zhang¹, Siwei Chen¹, Dan Zhang¹, Longfei Zhai², Jiafu Lin^{3,*} and Hui Lei^{1,*}

¹ School of Pharmacy, Southwest Medical University, Luzhou 646000, China; jiangly06@163.com (L.J.); tengbaorui01@163.com (B.T.); myzhang65@163.com (M.Z.); chensiwei2021@swmu.edu.cn (S.C.); zhangdan@swmu.edu.cn (D.Z.)

² Antibiotics Research and Re-Evaluation Key Laboratory of Sichuan Province, Sichuan Industrial Institute of Antibiotics, Chengdu University, Chengdu 610106, China; z960306@163.com

³ School of Pharmacy, Chengdu University, Chengdu 610106, China

* Correspondence: linjiafu@cdu.edu.cn (J.L.); huilei@swmu.edu.cn (H.L.); Tel.: +86-0830-3162291 (H.L.)

Abstract: Chemical epigenetic cultivation of the sponge-derived fungus *Pestalotiopsis* sp. SWMU-WZ04-1 contributed to the identification of twelve polyketide derivatives, including six new pestalotiopols E–J (1–6) and six known analogues (7–12). Their gross structures were deduced from 1D/2D NMR and HRESIMS spectroscopic data, and their absolute configurations were further established by circular dichroism (CD) Cotton effects and the modified Mosher’s method. In the bioassay, the cytotoxic and antibacterial activities of all compounds were evaluated. Chlorinated benzophenone derivatives 7 and 8 exhibited inhibitory effects on *Staphylococcus aureus* and *Bacillus subtilis*, with MIC values varying from 3.0 to 50 µg/mL. In addition, these two compounds were cytotoxic to four types of human cancer cells, with IC₅₀ values of 16.2–83.6 µM. The result showed that compound 7 had the probability of being developed into a lead drug with antibacterial ability.

Keywords: *Pestalotiopsis* sp.; polyketide; sponge-derived fungus; antibacterial activity; cytotoxicity



Citation: Jiang, L.; Teng, B.; Zhang, M.; Chen, S.; Zhang, D.; Zhai, L.; Lin, J.; Lei, H. Pestalotiopols E–J, Six New Polyketide Derivatives from a Marine Derived Fungus *Pestalotiopsis* sp. SWMU-WZ04-1. *Mar. Drugs* **2024**, *22*, 15. <https://doi.org/10.3390/md22010015>

Academic Editor: Bin Yang

Received: 29 November 2023

Revised: 23 December 2023

Accepted: 23 December 2023

Published: 26 December 2023



Copyright: © 2023 by the authors. Licensee MDPI, Basel, Switzerland. This article is an open access article distributed under the terms and conditions of the Creative Commons Attribution (CC BY) license (<https://creativecommons.org/licenses/by/4.0/>).

1. Introduction

Marine fungi provide a prospective source for the discovery of novel drug leads [1]. Traditional methods used in the investigation of marine fungi mainly focus on sample collection, the cultivation of fermentation broth, and mycelium. However, it is becoming difficult to discover novel structurally and biologically active metabolites using these traditional methods, but the development of genetic technology can assist [2]. Research findings demonstrate that a large portion of gene clusters are silenced under standard fermentation conditions [3–5]. To explore these potential secondary metabolites, activation of silent biosynthetic gene clusters has become an important strategy. At present, the silent gene clusters have been activated through multiple strategies, such as the OSMAC strategy [6–10], epigenetic modification [6,11,12], and genome mining. Of these, the chemical epigenetic strategy has proved to be an effective strategy for enhancing cryptic secondary metabolites [13].

During our ongoing efforts to discover more new and biologically active secondary metabolites from sponge-derived fungi, we applied the “epigenetic modification” strategy to the investigation of *Pestalotiopsis* sp., including 5-aza-2-deoxycytidine and suberoylanilide hydroxamic acid (SAHA). During this study, six new polyketide derivatives, pestalotiopols E–J (1–6), and six known analogues (7–12) (Figure 1), pestalochloride E (7) [14], (±)-pestalochloride D (8) [15], 3,4-dihydro-4, 6, 8-trihydroxy-1(2H)-naphthalenone (9) [16], isosclerone (10) [17], isobenzofuranyl derivative (11) [18], and (R)-3-hydroxy-1-[(S)-4-hydroxy-1,3-dihydroisobenzofuran-1-yl] butan-2-one (12) [19], were obtained from sponge-derived fungi *Pestalotiopsis* sp. ¹H and ¹³C assignments of the

pestalotiopols E–J (1–6) were accomplished, the absolute configurations of the compounds were determined by CD techniques, and furthermore, the biological activities of the separated organic molecules were assessed.

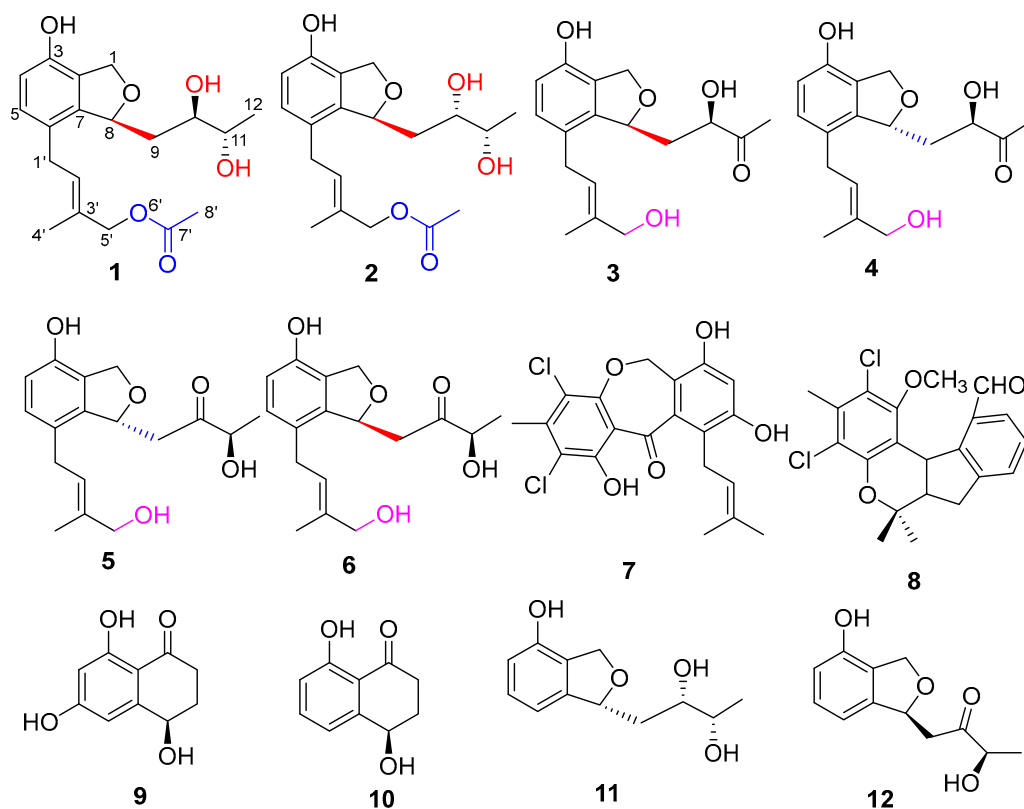


Figure 1. Chemical structures of compounds 1–12.

2. Results

Compound 1 appeared as a white solid, and its molecular formula was $C_{19}H_{26}O_6$, whose quasi-molecular ion peak was located at m/z 373.1635 $[M + Na]^+$ by HRESIMS. The 1H NMR spectrum (Table 1) showed two aromatic proton signals [δ_H 6.60 (d, $J = 8.1$ Hz, H-4), 6.87 (d, $J = 8.1$ Hz, H-5)], which belong to a 1,2,3,4-tetrasubstituted benzene, and one olefinic proton signal [δ_H 5.57 (brt, $J = 7.2$ Hz, H-2')]. The ^{13}C NMR spectrum of compound 1 showed 19 carbon resonances (Table 1), involving three CH_3 , four CH_2 , three sp^2 -CH carbons, and five not-containing proton carbons. One carbonyl carbon was proposed based on resonances at δ_C 172.8, and five oxygenated carbon signals at δ_C 71.0, 71.0, 71.7, 73.3, 82.3. The 1H NMR data was initially analyzed, and it was found that 1 had similar structural characteristics to heterocornol L [20]. The major difference was that a carbonyl signal was missing and an oxygenated methine was present in 1. This was proved by the HMBC correlations between H-10 (δ_H 3.71) and C-11 (δ_C 71.7), C-9 (δ_C 39.1), and C-12 (δ_C 18.9). The location of the vicinal diol side chain was confirmed by HMBC correlations from H-8 (δ_H 5.53) to C-7 (δ_C 143.4.), C-6 (δ_C 125.9), C-10 (δ_C 73.3), C-1 (δ_C 71.0), and 1H - 1H COSY correlations of H-8/H-9/H-10/H-11/H-12 (Figure 2). Furthermore, HMBC correlations found H-1' (δ_H 3.27) to C-5' (δ_C 71.0), C-2' (δ_C 128.8), C-3' (δ_C 132.3), and C-7 (δ_C 143.4), together with 1H - 1H COSY correlations located connections from H-1'/H-2' suggested the existence of 5'-O-acetyl isoamylenyl group located at C-6 in 1 (Figure 2). Therefore, the planar structure of 1 was established.

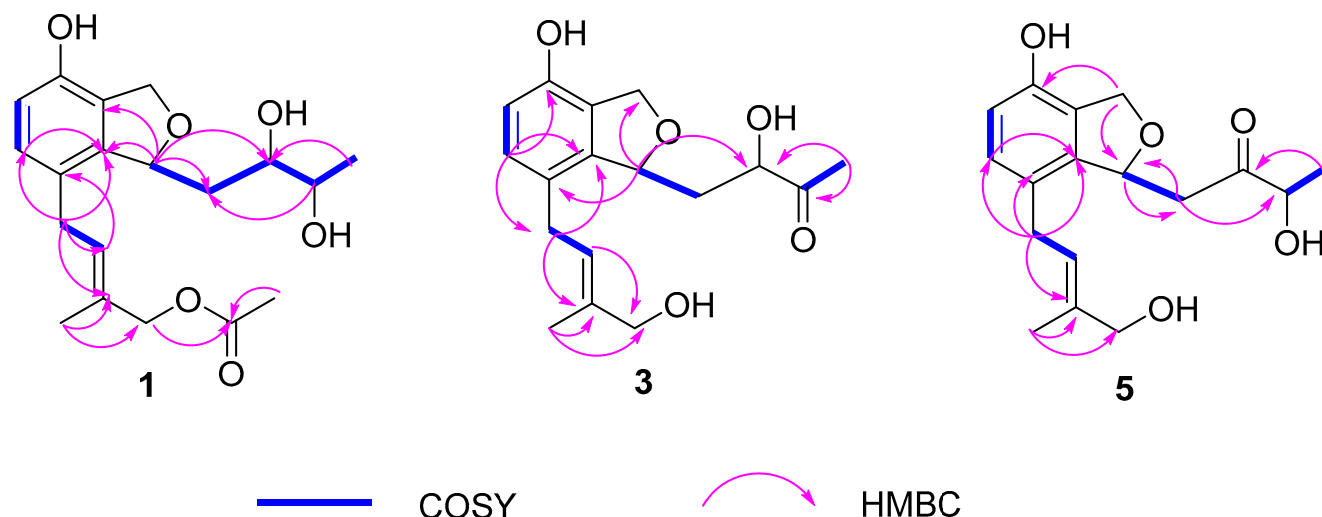


Figure 2. COSY and key HMBC correlations of 1, 3, 5.

To establish its relative configuration, the NOESY spectrum of **1** was performed; unfortunately, the NOESY spectrum of **1** was not useful for the assignment of the relative configuration at C-10 and C-11. According to the previously reported [21–24], in *rythron* vicinal diols ($J > 4.0$ Hz), the value of the coupling constant of the methine hydrogens was larger than 4 Hz, while in *threo* ones ($J < 2.0$ Hz), it is smaller than 2 Hz. On this account, consistent with the known pyriculin A and B [25] ($J = 3.7/3.8$ Hz), heterocornol I [20], indicating that the configurations of C-10 and C-11 in **1** ($J = 4.7$ Hz) were suggested as *erythro*. The absolute configuration of **1** (8*S*,10*R*,11*S*) was elucidated from the observed positive Cotton effect at 210 nm and positive Cotton effect at 313 nm in the CD and Mo₂(AcO)₄-induced CD spectra of **1**, respectively (Figure 3) [19].

Table 1. ¹H and ¹³C NMR data of compounds 1–3 in CD₃OD.

No.	δ_C , Type	1		2		3	
		δ_C , Type	δ_H (J in Hz)	δ_C , Type	δ_H (J in Hz)	δ_C , Type	δ_H (J in Hz)
1	71.0, CH		5.04, dd (12.3, 2.7) 4.95, d (12.3)	69.6, CH	5.08, dd (12.2, 2.6) 4.99, d (12.2)	71.2, CH	5.06, dd (12.2, 2.7) 4.96, d (12.2)
2	126.0, C			124.5, C		126.1, C	
3	151.1, C			149.9, C		151.2, C	
4	115.4, CH		6.60, d (8.1)	114.1, CH	6.63, d (8.0)	115.6, CH	6.61, d (8.2)
5	130.4, CH		6.87, d (8.1)	129.2, CH	6.88, d (8.0)	130.7, CH	6.89, d (8.2)
6	125.9, C			124.5, C		126.5, C	
7	143.4, C			141.6, C		142.8, C	
8	82.3, CH		5.53, brd (10.4)	83.4, CH	5.48, brd (10.2)	81.5, CH	5.51, m
9	39.1, CH ₂	1.83, ddd (14.3, 10.4, 2.0) 1.62, ddd (14.3, 10.4, 2.2) 3.71, ddd (10.4, 4.7, 2.1)	37.3, CH ₂	2.11, ddd (14.8, 3.9, 2.4) 1.70, dd (14.8, 6.0) 3.69, m	39.7, CH ₂	1.87, ddd (14.5, 4.9, 2.4) 1.90, ddd (14.5, 9.8, 7.1) 4.35, dd (9.9, 2.9)	
10	73.3, CH		74.4, CH	3.69, m	76.5, CH		
11	71.7, CH		69.9, CH	3.75, qd (6.2, 1.6)	213.5, C		
12	18.9, CH ₃		17.3, CH ₃	1.19, d (6.2)	25.8, CH ₃		
1'	31.0, CH ₂	3.27, dd (16.0, 7.0)	29.8, CH ₂	3.30, dd (16.0, 7.0)	31.2, CH ₂	2.18, s 3.24, dd (16.0, 6.9) 3.35, dd (16.0, 7.4) 5.30, t (7.6)	
2'	128.8, CH		127.3, CH	5.54, d (7.1)	127.1, CH		
3'	132.3, C		131.0, C		136.6, C		
4'	14.3, CH ₃	1.75, s	12.6, CH ₃	1.75, s	21.5, CH ₃	1.80, s	
5'	71.0, CH ₂	4.48, s	62.8, CH ₂	4.69, s	61.4, CH ₂	4.19, d (12.2), 4.20, d (12.2),	
7'	172.8, C		171.5, C				
8'	20.8, CH ₃	2.03, s	20.2, CH ₃	2.05, s			

Compound **2** was purified as a white solid with the molecular formula C₁₉H₂₆O₆, determined from the HRESIMS data. The NMR data of **2** were very similar to those of **1**, which manifests that both of them had the same planar structures. Compared with compound **1**, the configuration at C-10 and C-11 in the vicinal diol side chain was discrepant, which was proved by the chemical shifts of C-8 ($\Delta\delta_C$ 1.1 ppm), C-9 ($\Delta\delta_C$ −1.8 ppm), C-10 ($\Delta\delta_C$ 1.1 ppm), and C-11 ($\Delta\delta_C$ −1.8 ppm). According to the chemical shift of C-10 (δ_C 74.4)

and C-11 (δ_C 69.9) [26], and the coupling constant between H-10 and H-11 (1.6 Hz), the configuration of C-10 and C-11 was inferred to be *threo*. We speculated that **2** had the same configuration at C-8 (8*S*) as **1** according to their closely similar CD spectrum. The absolute configuration of C-10,11-diols in **2** was determined by $\text{Mo}_2(\text{AcO})_4$ -induced CD (Figure 3).

In order to further confirm the absolute configuration of **2**, the modified Mosher's method was performed (**2a** and **2b**) [27–30] (Figures S36 and S37). Treatment of **2** with [(*S*)-MTPA] and (*R*)-MTPA gave (*S*)-MTPA ester (**2a**) and (*R*)-MTPA ester (**2b**), respectively. The $\Delta\delta$ ($\delta_S - \delta_R$) values of **2a** and **2b** established the absolute configuration of C-10 and C-11 in **2**. Thus, compound **2** was assigned and named pestalotiopol F.

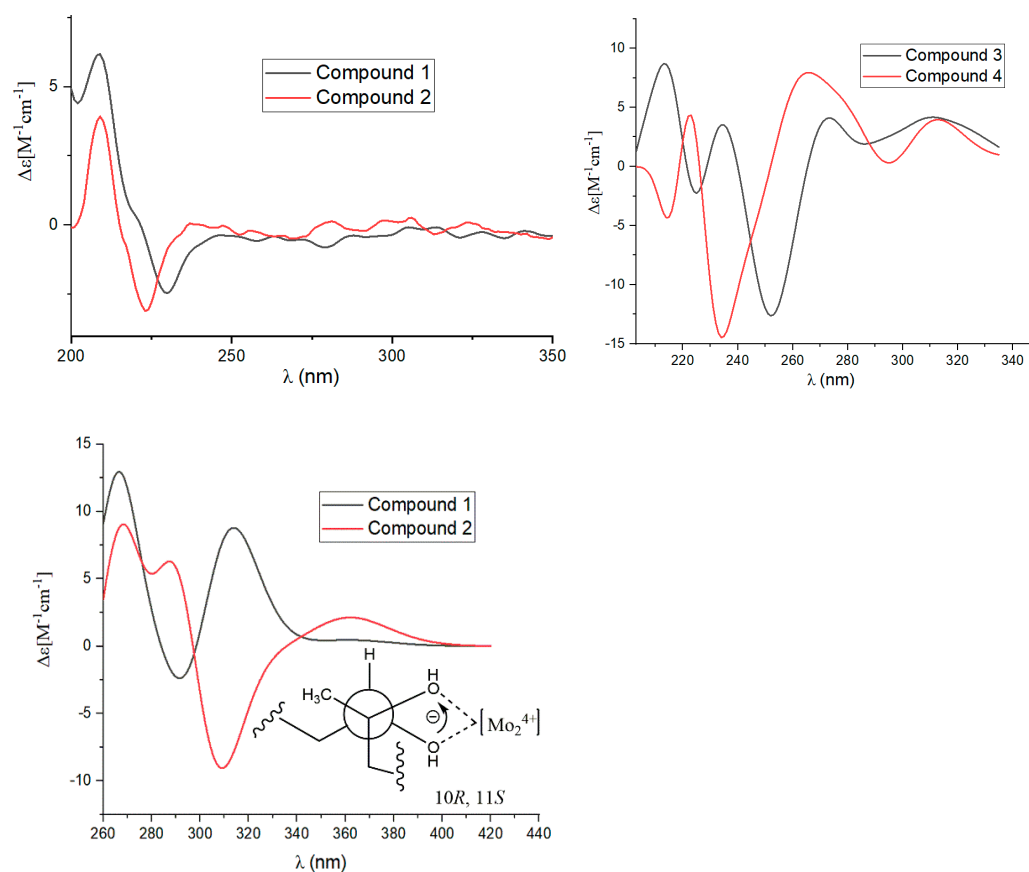


Figure 3. CD spectra of **1–4** as well as $\text{Mo}_2(\text{AcO})_4$ -induced CD spectra **1–2**.

Compound **3** appeared as a white solid, and the molecular formula was determined to be $\text{C}_{17}\text{H}_{22}\text{O}_5$. Analyses of the 1D/2D NMR data of **3** suggested that compound **3** was similar to vaccinol H [31]. One additional hydroxymethyl group (δ_C 61.4) was observed, which was established by HMBC correlations from H-2' (δ_H 5.30) to C-7 (δ_C 142.8), C-1' (δ_C 31.2), C-5' (δ_C 61.4), and C-6 (δ_C 126.5), from H-5' (δ_H 4.19/4.20) to C-4' (δ_C 21.5), C-3' (δ_C 136.6), and C-2' (δ_C 127.1). In terms of the positive Cotton effect at 212 nm and the biosynthetic pathway, along with the similar NMR data between vaccinol H and **3**, the configuration of **3** was confirmed to be 8*R*, 10*R*. The CD spectrum of (8*R*, 10*R*)-**3** helped reconfirm the configuration of **3** (Figure 3).

Compound **4** is presented as a white solid with a molecular formula of $\text{C}_{17}\text{H}_{22}\text{O}_5$, with its excimer ion peak located at m/z 307.1532 $[\text{M} + \text{H}]^+$. The NMR data indicated the same planar structure as **3** (Table 2). The differences between them were due to the variations in chemical shifts of C-8 (δ_C 81.5 in **3** vs. δ_C 81.2 in **4**) and C-9 (δ_C 39.7 in **3** vs. δ_C 44.3 in **4**). These results indicated both compounds differed in the relative configuration at C-8, which was similar to that of vaccinol H and vaccinol I. After contrasting the similarities in chemical shifts between **3** and **4**, and between vaccinol H and vaccinol I, together with

biogenetic considerations, we suggested that the absolute configuration of **4** was the 8*S*, 10*R* configuration. These assignments were further confirmed by the CD spectrum of **4** (Figure 3). Thus, we determined the structure of **4** and named it pestalotiopol H.

Table 2. ¹H and ¹³C NMR data of compounds **4–6** in CD₃OD.

No.	4		5		6	
	δ_C , Type	δ_H (J in Hz)	δ_C , Type	δ_H (J in Hz)	δ_C , Type	δ_H (J in Hz)
1	71.4, CH	5.05, dd (14.3, 2.2) 4.95, d (14.3)	70.1, CH	5.06, dd (12.3, 2.5) 4.96, d (12.3)	69.6, CH	5.03, dd (12.2, 2.3) 4.92, d (12.2)
2	126.1, C		125.0, C		124.7, C	
3	151.1, C		149.7, C		149.7, C	
4	115.7, CH	6.63, d (8.2)	114.3, CH	6.62, d (8.1)	114.1, CH	6.60, d (8.1)
5	130.8, CH	6.93, d (8.2)	129.3, CH	6.89, d (8.1)	129.2, CH	6.87, d (8.1)
6	126.4, C		125.6, C	5.31, t (7.8)	125.5, CH	5.31, t (7.8)
7	142.0, C		141.4, C		140.6, C	
8	81.2, CH	5.76, m	79.9, CH	5.74, m	79.4, CH ₂	5.72, m
9	44.3, CH ₂	2.91, d (9.6) 2.85, dd (16.2, 2.0) 4.23, q (7.0)	43.1, CH ₂	2.88, m	38.6, CH ₂	2.23, m
10	74.4, CH		211.8, C		211.5, CH	
11	212.7, C		74.7, CH	4.28, q (7.0)	73.3, CH	4.24, q (7.0)
12	19.5, CH ₃	1.29, d (7.0)	18.1, CH ₃	1.29, d (7.0)	17.9, CH ₃	1.33, d (7.0)
1'	31.2, CH ₂	3.21, m, 3.25, m	29.6, CH ₂	3.30, d (7.1)	29.6, CH ₂	3.30, d (7.1)
2'	124.8, CH	5.46, t (7.0)	125.0, CH	5.20, t (7.1)	125.3, CH	5.22, t (7.1)
3'	137, C		135.4, C		135.2, C	
4'	13.9, CH ₃	1.71, s	20.2, CH ₃	1.81, s	20.1, CH ₃	1.83, s
5'	68.6, CH ₂	3.95, s	60.0, CH ₂	4.16, s	60.0, CH ₂	4.16, s

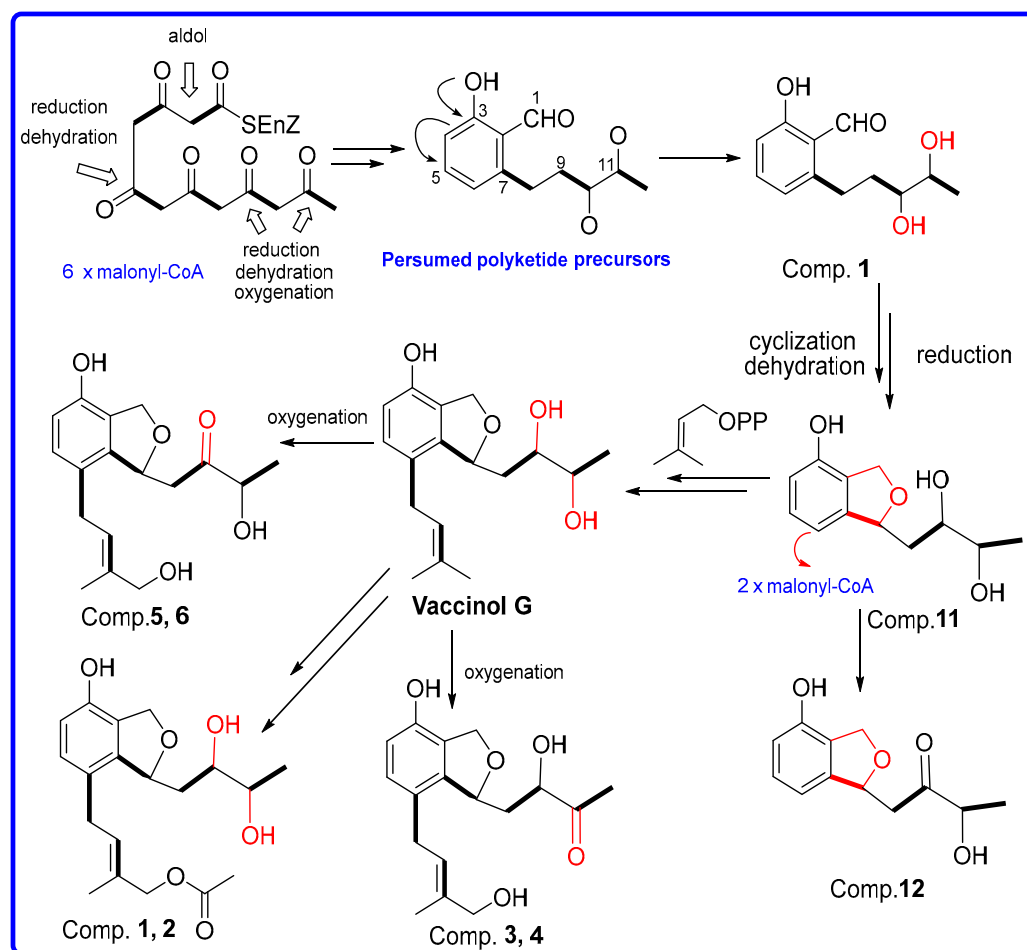
Compounds **5** and **6** were acquired as a mixture in a nearly 1:1 ratio, which was established by their HRESIMS and the ¹³C NMR data. The NMR data of **5** and **6** resembled those of **3** and **4**, except for a carbonyl group at C-10 (δ_C 211.8/211.5) in **5/6** and C-11 (δ_C 213.5/212.7) in **3/4**. Compared with **5**, the difference was that the chemical shift of C-8 (δ_C 79.4), C-9 (δ_C 38.6), and C-10 (δ_C 211.5) of **6** shifted to upfield (Δ 0.5 ppm, Δ 4.5 ppm, Δ 0.3 ppm), respectively. The conclusions mentioned above were confirmed by the HMBC correlations between H-8 and C-2/C-7/C-6/C-10, between H-5' and C-4'/C-3'/C-2', between H-1' and C-2'/C-3'/C-5/C-6, and the COSY cross peak of H-1'/H-2', H-8/H-9, and H-11/H-12. The absolute configurations of C-8 and C-11 in **5** and **6** were assigned 8*R*, 10*R*, and 8*S*, 10*R*, respectively, which were consistent with other analogs from the marine fungus *Pestalotiopsis vaccinii* [31]. Considering that two strains belong to the same genus, *Pestalotiopsis*, we proposed that they arose from the same biosynthetic pathway and shared the chiral center.

Biosynthetically, a precursor polyketide substance is commonly produced by microorganisms in the synthesis of aromatics and macrolides. Compounds (**1–6**, **11**, **12**) originated from malonyl-CoA by reduction, dehydration, cyclization, and oxidation to form the different polyketide precursors and subsequently formed compounds (**1–6**, **11**, **12**) after diverse transformations (Scheme 1).

In the present study, polyketide derivatives **1–12** were evaluated for their cytotoxic activities via MTT assay (Table 3). The cytotoxicity results demonstrated that compound **7** was mildly cytotoxic to HepG2, with IC₅₀ values of 16.2 μ M; the IC₅₀ values of **8**, which was weakly cytotoxic to human cancer cells, ranged from 34.8 to 63.1 μ M; unfortunately, compounds **1–6**, at concentrations of 100 μ M, did not show cytotoxicity against these tumor cell lines. Bacteriostatic effects **1–12** were performed (Table 3). Compounds **7** and **8** showed antibacterial effects on *Staphylococcus aureus* and *Bacillus subtilis*, with MIC values varying from 3 to 50 mg/mL. No obvious bioactivities were found in the other compounds at 100 μ M or 100 mg/mL. The results showed that there was considerable potential to develop compound **7** as a lead drug with antimicrobial activity.

In order to further verify the activity of compounds **7** and **8** against HepG2, the anti-apoptotic protein Bcl-2 (PDB ID: 4LVT) was used as a target for molecular docking. Compounds **7** and **8** bound to ASN9, TRP192, ILE186, TRP141, PHE195, TRP141, LEU198, TYR199, and GLN187 residues and formed hydrogen bonds and non-polar interactions, respectively. Noticeably, the docking results showed that compounds **7** and **8** were well

matched in the docking body of 4LVT and had good interaction with 4LVT. The binding free energies of systems were negative (-5.11 kcal/mol and -6.87 kcal/mol, respectively), indicating that the binding of proteins and small molecular ligands was a spontaneous process.



Scheme 1. Plausible biosynthetic pathway of compounds 1–6, 11, 12.

Table 3. Antibacterial activities and cytotoxicity of 1–12.

Comp.	Cytotoxicity (IC ₅₀ in μ M)				Antibacterial Activities (MIC μ g/mL)			
	H1975	7860	Hela	HepG2	<i>B. subtilis</i>	<i>S. aureus</i>	<i>E. coli</i>	<i>C. albicans</i>
1	>100	>100	>100	>100	>100	>100	>100	>100
2	>100	>100	>100	>100	>100	>100	>100	>100
3	>100	>100	>100	>100	>100	>100	>100	>100
4	>100	>100	>100	>100	>100	>100	>100	>100
5	>100	>100	>100	>100	>100	>100	>100	>100
6	>100	>100	>100	>100	>100	>100	>100	>100
7	83.6	>100	63.5	16.2	3.0	3.0	>100	>100
8	>100	63.1	45.0	34.8	50.0	50.0	50.0	>100
9	>100	>100	>100	>100	>100	>100	>100	>100
10	>100	>100	>100	>100	>100	>100	>100	>100
11	>100	>100	>100	>100	>100	>100	>100	>100
12	>100	>100	>100	>100	>100	>100	>100	>100
Adriamycin	1.48	2	2.6	2.2				
^a Ciprofloxacin					0.25 ^a	0.13 ^a	0.13 ^a	
^b Amphotericin								1.0 ^b

^a, Ciprofloxacin was used as a positive control against bacteria; ^b, Amphotericin was used as a positive control against fungi.

3. Materials and Methods

3.1. General Experimental Procedures

An MCP500 polarimeter (Anton) was used to record optical rotations in CH₃OH. IR and HRESIMS were performed on a Shimadzu IR and a Bruker maXis TOF-Q mass spectrometer, respectively. Two different Bruker spectrometers (AVANCE III-400 and AV-600) were used for the NMR data collection, and the NMR data were recorded using TMS as an internal standard, δ in ppm rel at 25 °C. Column chromatography involved normal-phase silica gel (100–300 mesh), Sephadex LH-20 (MeOH), and reversed-phase YMC ODS-A (50 μ m) being used, while precoated silica gel GF254 plates (0.20–0.25 mm in thickness) were used for thin-layer chromatography (TLC) analyses, and the spots were visualized by UV light (254 nm) and colored by spraying heated silica gel plates with 10% H₂SO₄ in ethanol. Preparative HPLC was conducted on a SAIPURUISHE system equipped with a UV detector, an ODS column (YMC-5 μ m, ODS-A, 250 mm \times 10 mm), a flow rate of 2.0 mL/min, and a column temperature of 25 °C. Circular dichroism (CD) spectra were recorded on a Chirascan circular dichroism spectrometer.

3.2. Fungal Material

The strain (SWMU-WZ04-1) was obtained from the sponge collected on Weizhou Island, China, and identified as *Pestalotiopsis* sp. SWMU-WZ04-1 by sequence alignment of the 18S rRNA gene. During its initial growth stage on a PDA plate, the mycelium of *Pestalotiopsis* sp. SWMU-WZ04-1 showed a french grey, which gradually transitioned to a brown color. As growth progressed, the mycelium produced conidia along with small oil droplets on the surface.

3.3. Fermentation, Extraction, and Isolation

The fungus SWMU-WZ04-1 was cultivated on a rice culture medium (200 g rice, 3% sea salt, 200 mL water, 10 μ M of 5-aza-2-deoxycytidine and suberoylanilide hydroxamic acid (SAHA), 120 flasks) for 40 days at a temperature of 28 °C. After fermentation, the fungal culture was exhaustively extracted with EtOAc to obtain a crude extract (48.9 g).

The crude extract was fractionated on a normal-phase column using a stepped gradient elution with petroleum ether/EtOAc (30: 1 to 0: 1, *v/v*) to obtain 8 fractions (Fr.1–Fr.8). Fr.3 was applied to a normal-phase column (petroleum ether/EtOAc, 15:1-3:1) to obtain three subfractions (Frs. 3.1–3.3). Fr. 3.2 was purified with Sephadex LH-20 (MeOH) and further purified by HPLC eluting (MeOH/H₂O 60%) to obtain compounds **3** (8.0 mg) and **4** (3.0 mg). Fr. 3.3 was further separated by an ODS column eluting with MeOH/H₂O (60%) to obtain subfractions (Fr.3.3.1–Fr.3.3.4). Fr.3.3.2 was purified by Sephadex LH-20 column (MeOH) and HPLC (60%, MeOH/H₂O) to obtain **11** (6.0 mg) and **12** (5.0 mg). Fr. 4 was subjected to silica gel (petroleum ether-EtOAc, 3:1-0:1) and further separated by (70%, MeOH/H₂O) HPLC and Sephadex LH-20 (MeOH) to yield **1** (7.0 mg) and **2** (4.0 mg). Fr. 5 was applied by Sephadex LH-20 chromatography (MeOH) and HPLC (60% MeOH/H₂O) to afford **7** (10.0 mg) and **8** (3.0 mg). Fr. 6 was further divided into seven subfractions (Frs.6.1–6.7) by silica gel cc (CH₂Cl₂-Acetone, 6:1-0:1). Frs.6.3 was applied by Sephadex LH-20 (MeOH) and HPLC (H₂O/MeOH) to yield **5/6** (3.0 mg). Frs. 6.6 was applied by HPLC (MeOH/H₂O, 45%) to afford **9** (7.0 mg) and **10** (7.0 mg).

Pestalotiopol E (**1**): white solid; $[\alpha]_D^{25}$ –55 (c 0.3, MeOH); UV (MeOH) λ_{max} (log ϵ) 254 (2.24), 275 (3.28) nm; ¹H NMR and ¹³C NMR data, Table 1; HRESIMS *m/z* 373.1635 [M + Na]⁺ (calcd for C₁₉H₂₆NaO₆, 373.1632).

Pestalotiopol F (**2**): white solid; $[\alpha]_D^{25}$ –50 (c 0.4, MeOH); UV (MeOH) λ_{max} (log ϵ) 246 (3.18) nm; ¹H NMR and ¹³C NMR data, Table 1; HRESIMS *m/z* 373.1658 [M + Na]⁺ (calcd for C₁₉H₂₆NaO₆, 373.1645).

Pestalotiopol G (**3**): white solid; $[\alpha]_D^{25}$ –10 (c 0.4, MeOH); UV (MeOH) λ_{max} (log ϵ) 254 (2.60), 210 (3.36) nm; ¹H NMR and ¹³C NMR data, Table 1; HRESIMS *m/z* 305.1391 [M – H][–] (calcd for C₁₇H₂₁O₅, 305.1409).

Pestalotiopol H (4): white solid; $[\alpha]_D^{25} +14$ (c 0.2, MeOH); UV (MeOH) λ_{\max} (log ϵ) 246 (3.23), 210 (3.56) nm; ^1H NMR and ^{13}C NMR data, Table 2; HRESIMS m/z 307.1532 $[\text{M} + \text{H}]^+$ (calcd for $\text{C}_{17}\text{H}_{23}\text{O}_5$, 307.1525).

Pestalotiopol I and J (5/6): white solid; UV (MeOH) λ_{\max} (log ϵ) 254 (3.56) nm; ^1H NMR and ^{13}C NMR data, Table 2; HRESIMS m/z 307.1533 $[\text{M} + \text{H}]^+$ (calcd for $\text{C}_{17}\text{H}_{23}\text{O}_5$, 307.1526).

3.4. $\text{Mo}_2(\text{AcO})_4$ -Induced CD

The $\text{Mo}_2(\text{AcO})_4$ solution was prepared with DMSO; subsequently, compounds **1** and **2** were added to the stock solution, respectively. The CD spectra of compounds **1** and **2** were recorded immediately after every 10 min for 30 min to form stationary $\text{Mo}_2(\text{AcO})_4$ -induced CD spectra [32].

3.5. Preparation of (S)- and (R)-MTPA Esters of **2**

Each of duplicate **2** (1.7 mg) in 0.3 mL anhydrous pyridine- d_6 in NMR tubes was reacted with (S)- and (R)-MTPA (160 μL , for **2**), respectively. The reaction was performed at 50 °C for 15 h. Then, the ^1H NMR data of the (S)- and (R)-MTPA esters were obtained without purification [33–36].

3.6. Cytotoxicity Assay

The MTT method was applied to analyze the cytotoxicity of compounds **1–12** against four cancer cell lines, involving (7860), (HepG2), (H1975), and (Hela). The MTT assay was depicted as a previously used method [37]. The cells were seeded in complete medium per well within a 96-well plate. The cells were incubated at 37 °C for 12–24 h to facilitate adherent cell growth. Following this, compounds **1–12** solutions were added, and cells were cultured for 48 h. Subsequently, MTT solution was introduced into the wells and incubated for 4 h at 37 °C. DMSO was added to each well after the cell medium was discarded. The absorbance was measured at a wavelength of 570 nm.

3.7. Antimicrobial Assay

The antimicrobial assay against three bacteria (*Bacillus subtilis*, *Staphylococcus aureus*, and *Escherichia coli*) and one fungus (*Candida albicans*) was assessed for adopting the microbroth dilution reported previously [38]. The MIC was defined as the lowest concentration of the antimicrobial agent that completely inhibited the visual growth of an organism. Ciprofloxacin and amphotericin B were used as positive controls against bacteria and fungi, respectively.

3.8. Molecular Docking

The molecular docking of compounds **7** and **8** was performed (Figure 4). The initial models for Bcl-2 (PDB ID:4LVT) was gained from the Protein Data Bank (<http://www.rcsb.org>, accessed on 16 November 2023). The 3D structures of compounds **7** and **8** were obtained from ChemBio 3D Ultra 14.0. AutoDock Vina (Center for Computational Structural Biology, La Jolla, the US, accessed on 16 November 2023), and AutoDockTools-1.5.6 were used to generate docking input files [39]. The docking results were then analyzed for interaction patterns using PyMOL 2.3.0.

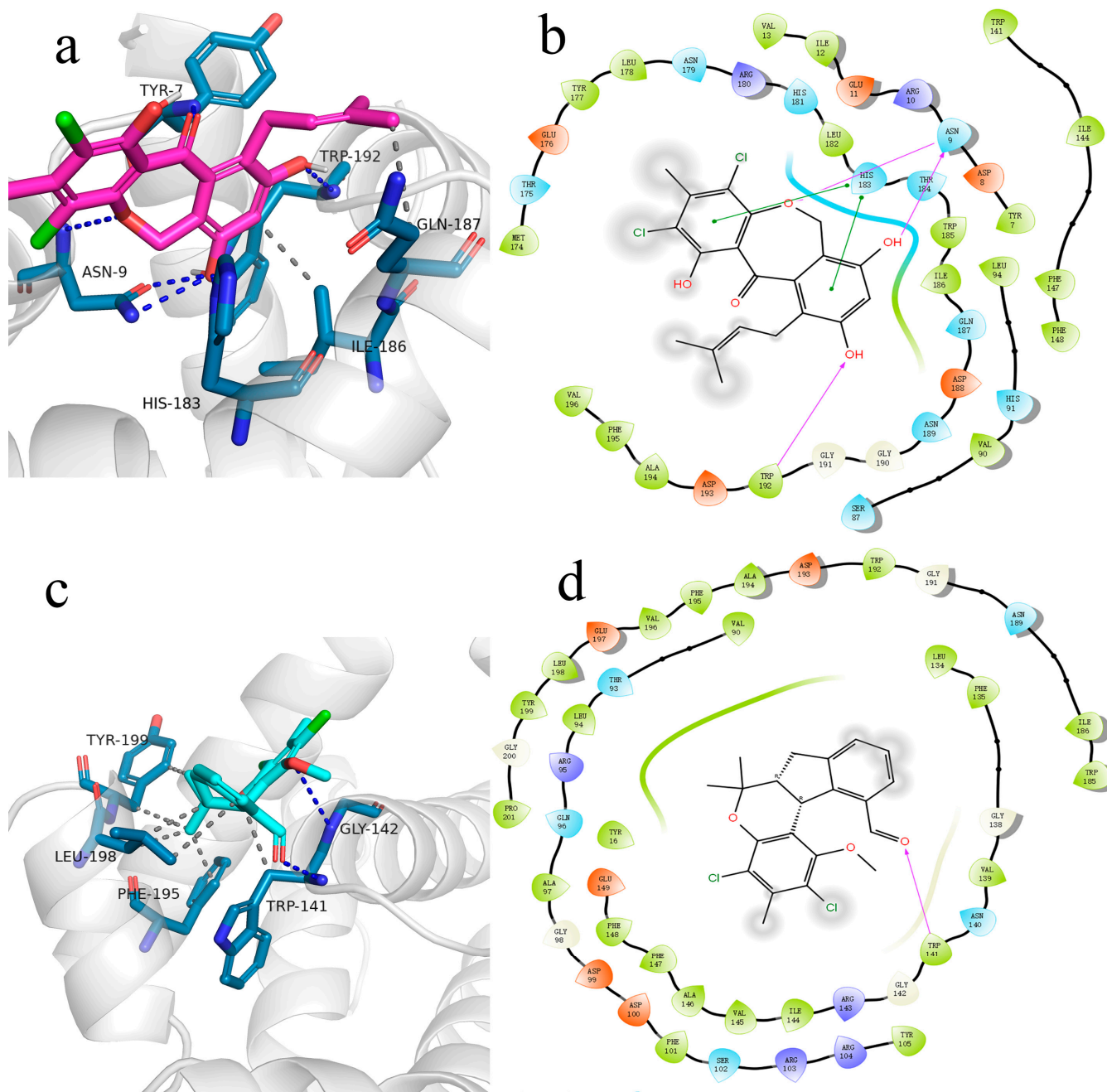


Figure 4. Representative docking poses of compounds 7 and 8 bound to Bcl-2 (PDB ID: 4LVT). The intermolecular interactions between Bcl-2 (PDB ID: 4LVT) and compounds 7 and 8 are as depicted in the maps (a,c) and the maps (b,d).

4. Conclusions

In summary, we identified six new polyketide derivatives (1–6) and six known compounds (7–12) that were produced by chemical epigenetic cultivation. The absolute configurations of 1 and 2 were further established by circular dichroism (CD) cotton effects and the modified Mosher's method. Compounds 7 and 8 manifested antibacterial activities against *Staphylococcus aureus* and *Bacillus subtilis*, with MIC values varying from 3 to 50 mg/mL. The result of the analysis showed that the potential to develop compound 7 as a lead drug with antibacterial activity is quite high. In addition, although the cytotoxic and antibacterial activities of compounds 7 and 8 were evaluated, the detailed mechanism of action is still undefined; thus, further studies are needed.

Supplementary Materials: The following supporting information can be downloaded at <https://www.mdpi.com/article/10.3390/md22010015/s1>, Figures S1–S35: 1D, 2D NMR, and HRESIMS spectra of compounds 1–6. Figures S36,S37: ¹H NMR spectrum of the compounds 2a,2b; Figure S38: The $\Delta\delta$ (δ_S – δ_R) values from the (S)- and (R)-MTPA esters of 2.

Author Contributions: L.J. and H.L. performed experiments and writing—original draft preparation. L.Z. and J.L. contributed the isolation of the fungal strain. M.Z. and S.C. contributed to this work through bioassay experiments. B.T. performed molecular docking. D.Z. revised the manuscript. All authors have read and agreed to the published version of the manuscript.

Funding: This work was funded by the Department of Science and Technology of Sichuan Province (2022NSFSC0109), the Sichuan Science and Technology Program (2022YFS0624), the Open Project of Sichuan Industrial Institute of Antibiotics, Chengdu University (ARRLKF20-04), the Applied Basic Research Fund of the Second People’s Hospital of Deyang City-Southwest Medical University (2022DYEXNYD004), and the Sichuan Traditional Chinese Medicine Administration (2023zd008).

Institutional Review Board Statement: Not applicable.

Data Availability Statement: The data presented in this study are available in the main text and the Supplementary Materials of this article.

Conflicts of Interest: The authors declare no conflict of interest.

References

1. Zhang, B.; Zhang, T.; Xu, J.; Lu, J.; Qiu, P.; Wang, T.; Ding, L. Marine sponge-associated fungi as potential novel bioactive natural product sources for drug discovery. *Mini Rev. Med. Chem.* **2020**, *20*, 1966–2010. [[CrossRef](#)] [[PubMed](#)]
2. Pan, R.; Bai, X.L.; Chen, J.W.; Zhang, H.W.; Wang, H. Exploring structural diversity of microbe secondary metabolites using OSMAC strategy: A literature review. *Front. Microbiol.* **2019**, *10*, 294. [[CrossRef](#)] [[PubMed](#)]
3. Zhang, X.; Hindra, Elliot, M.A. Unlocking the trove of metabolic treasures: Activating silent biosynthetic gene clusters in bacteria and fungi. *Curr. Opin. Microbiol.* **2019**, *51*, 9–15. [[CrossRef](#)] [[PubMed](#)]
4. Jiang, P.; Fu, X.J.; Niu, H.; Chen, S.W.; Liu, F.F.; Luo, Y.; Zhang, D.; Lei, H. Recent advances on *Pestalotiopsis* genus: Chemistry, biological activities, structure–activity relationship, and biosynthesis. *Arch. Pharmacol. Res.* **2023**, *46*, 449–499. [[CrossRef](#)] [[PubMed](#)]
5. Wang, X.R.; Filho, J.G.S.; Hoover, A.R.; King, J.B.; Ellis, T.K.; Powell, D.R.; Cichewicz, R.H. Chemical epigenetics alters the secondary metabolite composition of guttate excreted by an atlantic-forest-soil-derived *Penicillium citreonigrum*. *J. Nat. Prod.* **2010**, *73*, 942–948. [[CrossRef](#)] [[PubMed](#)]
6. Cristina, P.R.; Aleu, J.; Rosa, D.P. Cryptic metabolites from marine-derived microorganisms using OSMAC and epigenetic approaches. *Mar. Drugs* **2022**, *20*, 84.
7. Li, W.; Ding, L.J.; Wang, N.; Xu, J.Z.; Zhang, W.Y.; Zhang, B.; He, S.; Wu, B.; Jin, H.X. Isolation and characterization of two new metabolites from the sponge-derived fungus *Aspergillus* sp. LS34 by OSMAC approach. *Mar. Drugs* **2019**, *17*, 283. [[CrossRef](#)]
8. Zang, Y.; Gong, Y.H.; Gong, J.J.; Liu, J.J.; Chen, C.M.; Gu, L.H.; Zhou, Y.; Wang, J.P.; Zhu, H.C.; Zhang, Y.H. Fungal polyketides with three distinctive ring skeletons from the fungus *Penicillium canescens* uncovered by OSMAC and molecular networking strategies. *J. Org. Chem.* **2020**, *85*, 4973–4980. [[CrossRef](#)]
9. Victor, R.M.A.; Monica, T.M.; Cristina, C.; Antonio Hernandez, D.; Antonio, F.M.; Jose, M.S.L. OSMAC approach and cocultivation for the induction of secondary metabolism of the fungus *Pleotrichocladium opacum*. *ACS Omega* **2023**, *8*, 39873–39885.
10. Victor Rodriguez, M.A.; Francisco Romero, M.; Cristina, C.; Antonio Hernandez, D.; Antonio Fernandez, M.; Jose, M.; Sanchez, L. Induction of new aromatic polyketides from the marine actinobacterium *Streptomyces griseorubiginosus* through an OSMAC approach. *Mar. Drugs* **2023**, *21*, 526.
11. Liu, S.L.; Zhou, L.; Chen, H.P.; Liu, J.K. Sesquiterpenes with diverse skeletons from histone deacetylase inhibitor modified cultures of the basidiomycete *Cyathus stercoreus* (Schwein.) De Toni HFG134. *Phytochemistry* **2022**, *195*, 113048. [[CrossRef](#)] [[PubMed](#)]
12. Zhang, W.F.; Li, J.Y.; Wei, C.W.; Deng, X.L.; Xu, J. Chemical epigenetic modifiers enhance the production of immunosuppressants from the endophytic fungus *Aspergillus fumigatus* isolated from *Cynodon dactylon*. *Nat. Prod. Res.* **2022**, *36*, 4481–4485. [[CrossRef](#)] [[PubMed](#)]
13. Xue, M.Y.; Hou, X.W.; Fu, J.J.; Zhang, J.Y.; Wang, J.C.; Zhao, Z.T.; Xu, D.; Lai, D.E.; Zhou, L.G. Recent advances in search of bioactive secondary metabolites from fungi triggered by chemical epigenetic modifiers. *J. Fungi* **2023**, *9*, 172. [[CrossRef](#)] [[PubMed](#)]
14. Xing, Q.; Gan, L.S.; Mou, X.F.; Wang, W.; Wang, C.Y.; Wei, M.Y.; Shao, C.L. Isolation, resolution and biological evaluation of pestalochlorides E and F containing both point and axial chirality. *RSC Adv.* **2016**, *6*, 22653–22658. [[CrossRef](#)]
15. Wei, M.Y.; Li, D.; Shao, C.L.; Deng, D.S.; Wang, C.Y. (±)-Pestalochloride D, an antibacterial racemate of chlorinated benzophenone derivative from a soft coral-derived fungus *Pestalotiopsis* sp. *Mar. Drugs* **2013**, *11*, 1050–1060. [[CrossRef](#)] [[PubMed](#)]
16. Iwasaki, S.; Muro, H.; Sasaki, K.; Nozoe, S.; Okuda, S.; Sato, Z.J. Isolations of phytotoxic substances produced by *pyricularia oryzae* cavara. *Tetrahedron Lett.* **1973**, *37*, 3537–3542. [[CrossRef](#)]
17. Venkatasubbaiah, P.; Chilton, W.S. Toxins produced by the dogwood anthracnose fungus *Discula* sp. *J. Nat. Prod.* **1991**, *54*, 1293–1297. [[CrossRef](#)]

18. Bouillant, M.L.; Bernilion, J.; Favre-Bonvin, J.; Salin, N. New hexaketides related to sordariol in *Sordaria macrospora*. *Z. Naturforschung C* **1989**, *44*, 719. [[CrossRef](#)]
19. Kesting, J.R.; Olsen, L.; Staerk, D.; Tejesvi, M.V.; Kini, K.R.; Prakash, H.S.; Jaroszewski, J.W. Production of unusual dispiro metabolites in *Pestalotiopsis virgatula* endophyte cultures: HPLC-SPE-NMR, electronic circular dichroism, and time-dependent density-functional computation study. *J. Nat. Prod.* **2011**, *74*, 2206–2215. [[CrossRef](#)]
20. Lei, H.; Lin, X.P.; Han, L.; Ma, J.; Dong, K.L.; Wang, X.B.; Zhong, J.L.; Mu, Y.; Liu, Y.H.; Huang, X.S. Polyketide derivatives from a marine-sponge-associated fungus *Pestalotiopsis heterocornis*. *Phytochemistry* **2017**, *142*, 51–59. [[CrossRef](#)]
21. Jarvis, B.B.; Comezoglu, S.N.; Rao, M.M.; Pena, N.B. Isolation of macrocyclic trichothecenes from a large-scale extract of *Baccharis megapota*. *J. Org. Chem.* **1987**, *52*, 45–56.
22. Chen, X.W.; Li, C.W.; Cui, C.B.; Hua, W.; Zhu, T.J.; Gu, Q.Q. Nine new and five known polyketides derived from a deep sea-sourced *Aspergillus* sp. 16-02-1. *Mar. Drugs* **2014**, *12*, 3116–3137. [[CrossRef](#)] [[PubMed](#)]
23. Ayer, W.A.; Trifonov, L.S. Metabolites of *Peniophora polygonia*, part 2. Some aromatic compounds. *J. Nat. Prod.* **1993**, *56*, 85–89. [[CrossRef](#)]
24. Jarvis, B.B.; Wang, S.; Ammon, H.L. Trichoveroid stereoisomers. *J. Nat. Prod.* **1996**, *59*, 254–261. [[CrossRef](#)] [[PubMed](#)]
25. Masi, M.; Meyer, S.; Górecki, M.; Mandoli, A.; Bari, L.D.; Pescitelli, G.; Cimmino, A.; Cristofaro, M.; Clement, S. Pyricularins A and B, two monosubstituted hex-4-ene-2,3-diols and other phytotoxic metabolites produced by *Pyricularia grisea* isolated from buffelgrass (*Cenchrus ciliaris*). *Chirality* **2017**, *29*, 726–736. [[CrossRef](#)] [[PubMed](#)]
26. Andolfi, A.; Cimmino, A.; Vurro, M.; Berestetskiy, A.; Troise, C.; Zonno, M.C.; Motta, A.; Evidente, A. Agropyrenol and agropyrenal, phytotoxins from *Ascochyta agropyrina* var. *nana*, a fungal pathogen of *Elitrigia repens*. *Phytochemistry* **2012**, *79*, 102–108. [[CrossRef](#)] [[PubMed](#)]
27. Hoye, T.R.; Jeffrey, C.S.; Shao, F. Mosher ester analysis for the determination of absolute configuration of stereogenic (chiral) carbinol carbons. *Nat. Protoc.* **2007**, *2*, 2451–2458. [[CrossRef](#)] [[PubMed](#)]
28. Ohtani, I.; Kusumi, T.; Kashman, Y.; Kakisawa, H. High-field FT NMR application of Mosher's method. The absolute configurations of marine terpenoids. *J. Am. Chem. Soc.* **1991**, *113*, 4092–4096. [[CrossRef](#)]
29. Kang, C.Q.; Guo, H.Q.; Qiu, X.P.; Bai, X.L.; Yao, H.B.; Gao, L.X. Assignment of absolute configuration of cyclic secondary amines by NMR techniques using Mosher's method: A general procedure exemplified with (-)-isoanabasine. *Magn. Reson. Chem.* **2006**, *44*, 20–24. [[CrossRef](#)]
30. Kusumi, T.; Ooi, T.; Ohkubo, Y.; Yabuuchi, T. The modified Mosher's method and the sulfoximine method. *Bull. Chem. Soc. Jpn.* **2006**, *79*, 965–980. [[CrossRef](#)]
31. Wang, J.F.; Wei, X.Y.; Qin, X.C.; Chen, H.; Lin, X.P.; Zhang, T.Y.; Yang, X.W.; Liao, S.R.; Yang, B.; Liu, J.; et al. Two new prenylated phenols from endogenous fungus *Pestalotiopsis vaccinii* of mangrove plant *Kandelia candel* (L.) Druce. *Phytochem. Lett.* **2015**, *12*, 59–62. [[CrossRef](#)]
32. Gu, C.Z.; Lv, J.J.; Zhang, X.X.; Qiao, Y.J.; Yan, H.; Li, Y.; Wang, D.; Zhu, H.T.; Luo, H.R.; Yang, C.R.; et al. Triterpenoids with promoting effects on the differentiation of PC12 cells from the steamed roots of *Panax notoginseng*. *J. Nat. Prod.* **2015**, *78*, 1829–1840. [[CrossRef](#)] [[PubMed](#)]
33. Jin, Y.; Aobulikasimu, N.; Zhang, Z.G.; Liu, C.B.; Cao, B.X.; Lin, B.; Guan, P.P.; Mu, Y.; Jiang, Y.; Han, L. Amycolasporins and dibenzoyls from lichen-associated *Amycolatopsis hippodromi* and their antibacterial and antiinflammatory activities. *J. Nat. Prod.* **2020**, *83*, 3545–3553. [[CrossRef](#)] [[PubMed](#)]
34. Ding, N.; Jiang, Y.; Han, L.; Chen, X.; Ma, J.; Qu, X.; Mu, Y.; Liu, J.; Li, L.; Jiang, C.; et al. Bafilomycins and odoriferous sesquiterpenoids from *Streptomyces albolongus* isolated from *Elephas maximus* feces. *J. Nat. Prod.* **2016**, *79*, 799–805. [[CrossRef](#)] [[PubMed](#)]
35. Burley, S.K.; Bhikadiya, C.; Bi, C.; Bittrich, S.; Chen, L.; Crichlow, G.V.; Christie, C.H.; Dalenberg, K.; Di Costanzo, L.; Duarte, J.M.; et al. RCSB Protein Data Bank: Powerful new tools for exploring 3D structures of biological macromolecules for basic and applied research and education in fundamental biology, biomedicine, biotechnology, bioengineering and energy sciences. *Nucleic Acids Res.* **2021**, *49*, D437–D451. [[CrossRef](#)] [[PubMed](#)]
36. Saito, T.; Itabashi, T.; Wakana, D.; Takeda, H.; Yaguchi, T.; Kawai, K.; Hosoe, T. Isolation and structure elucidation of new phthalide and phthalane derivatives, isolated as antimicrobial agents from *Emericella* sp. IFM57991. *J. Antibiot.* **2015**, *69*, 89–96. [[CrossRef](#)]
37. Su, B.N.; Park, E.J.; Mbwambo, Z.H.; Santarsiero, B.D.; Mesecar, A.D.; Fong, H.H.S.; Pezzuto, J.M.; Kinghorn, A.D. New chemical constituents of euphorbia quinquecostata and absolute configuration assignment by a convenient Mosher ester procedure carried out in NMR tubes. *J. Nat. Prod.* **2002**, *65*, 1278–1282. [[CrossRef](#)]
38. Rieser, M.J.; Hui, Y.H.; Rupprecht, J.K.; Kozlowski, J.F.; Wood, K.V.; McLaughlin, J.L.; Hanson, P.R.; Zhuang, Z.P.; Hoye, T.R. Determination of absolute configuration of stereogenic carbinol centers in annonaceous acetogenins by ¹H- and ¹⁹F-NMR analysis of Mosher ester derivatives. *J. Am. Chem. Soc.* **1992**, *114*, 10203–10213. [[CrossRef](#)]
39. Kouda, K.; Ooi, T.; Kusumi, T. Application of the modified Mosher's method to linear 1,3-diols. *Tetrahedron Lett.* **1999**, *40*, 3005–3008. [[CrossRef](#)]

Disclaimer/Publisher's Note: The statements, opinions and data contained in all publications are solely those of the individual author(s) and contributor(s) and not of MDPI and/or the editor(s). MDPI and/or the editor(s) disclaim responsibility for any injury to people or property resulting from any ideas, methods, instructions or products referred to in the content.